Bond model of steel reinforcement embedded in low binder concrete

Ricardo Bastos
ricardo.bastos@ist.utl.pt

Instituto Superior Técnico, Lisbon, Portugal
May 2022

Abstract

The present work presents a new bond model of steel reinforcement embedded in low binder concrete. The bond model was obtained through an empirical calibration process based on the results of the pull-out test campaigns from Louro (2014), Freitas (2016) and Pereira (2019). These results comprise data from 31 test series of 138 pull-out tests conducted with various concrete types. Furthermore, the specimens from these campaigns were emulated through the finite element modelling of the pull-out tests through the ATENA software. The finite element modelling of the local bond behaviour was produced through a phenomenological approach which enabled the comparison between experimental results and numerical results using the new bond model and the pre-existing ones of fib Model Code 2010, Louro (2014), Freitas (2016) and Pereira (2019). Subsequently, two beams were modelled to study the influence of the bond strength over the anchorage/lap-splice length.

The conclusions from this work were as follows: the calibration of a new bond model incorporated the influence of the bond-related parameters of bond index, bar diameter, packing density and recycled aggregate content. Moreover, it improved the bond strength prediction accuracy compared to previous models. The modelling performed for the pull-out test successfully simulated the local bond behaviour. The beam models revealed a linear relationship between the variation of bond strength and anchorage/lap-splice length. Lastly, the proper consideration of the bond strength capacity at anchorage zones can have an important effect on material savings and contribute to the construction industry's sustainability.

Keywords: Bond behaviour, pull-out test, low binder concrete, finite element analysis, anchorage length

INTRODUCTION

Framework

The present dissertation is centred on the bond behaviour of embedded steel reinforcement, with a special focus on using ecological concrete types involving recycled aggregates and low quantities of cement. The study of these types of concrete comes from the necessity to promote the sustainability of the construction industry, which can be achieved by the proper employment of materials with a lower ecological footprint.

Concrete is the most widely used construction material globally and a significant contributor to climate change. The Portland cement makes up 74 to 81% of the total CO2 emissions from concrete (Flower and Sanjayan 2007). Furthermore, cement production is the source of around 8% of the world's CO2 emissions. Currently, more than 4 billion tonnes of cement are produced worldwide, and global production is set to increase to 5 billion tonnes by the end of 2030 (Lehne and Preston 2018).

Moreover, due to the high percentage of coarse aggregate used in concrete (60 to 75% of the total concrete volume, according to Kosmatka *et al.* (1996)), a sustainable and economical source for obtaining high-quality aggregate is essential to the construction industry. Availability of high-quality aggregate sources close to growing urban centres, where the construction demand is high, might be limited; thus, recycled aggregates produced from the concrete remnants of construction and demolition waste is a potential solution to this problem. In this way, there is a potential to reduce aggregate costs as well as CO2 emissions associated with transportation. For the past years, the production of concrete using recycled materials has been increasingly encouraged. According to the European Aggregates Association, the yearly aggregate demand by weight surmounts 3 billion tonnes, with recycled aggregates only accounting for 8% of the total aggregate production, contrasting with the 87% generated from natural resources in quarries and pits.

Engineers considering the structural use of low quantities of binder and recycled aggregates to promote the sustainability of concrete construction need to understand the behaviour of these innovative concrete types and how it compares to ordinary concrete (OC). The bond between steel reinforcing bars and concrete has significant importance in the structural performance of concrete structures, both under ultimate and serviceability limit states. Therefore, it is necessary to know how the current design codes' recommendations can accurately predict the structural response of reinforced concrete members built using new materials such as low binder concrete (LBC) or low cement recycled aggregate concrete (LCRAC).

Goals

The target goals of the present work are the following:

• Calibration of a new local bond stress-slip model for steel reinforcement embedded in ordinary concrete, low binder concrete or low cement recycled aggregate concrete.

• Finite element modelling of the local bond behaviour by replicating the pull-out test specimens of Louro (2014), Freitas (2016) and Pereira (2019).

• Evaluation of the current bond models by comparing experimental and numerical results.

• FE modelling of structural members using the local bond model utilised in the pull-out numerical models to evaluate the bond behaviour of reinforcement with long embedded lengths and their performance at the anchorage zones.

CALIBRATION OF THE BOND STRESS-SLIP RELATIONSHIP

A calibration process of an optimized bond stress-slip model regarding the local bond behaviour in good bond conditions and with a pull-out ductile failure was performed by analysing the existing bond models presented by several authors and the data from the pull-out test experiments performed on reinforcement embedded in various concrete mixtures. The calibration process aimed to achieve an optimised bond stress-slip model capable of accurately predicting the local bond behaviour of ribbed bars embedded in OC, LBC and LCRAC mixtures.

The existing bond models analysed during the calibration process were those presented in *fib* Model Code 2010, Louro (2014), Freitas (2016) and Pereira (2019). Furthermore, the empirical evidence was provided by the data relative to the total of 138 pull-out tests performed separately by Louro (2014), Freitas (2016) and Pereira (2019). Ultimately, the bond-related parameters investigated during this operation were the concrete compressive strength, the bond index, the packing density, the bar diameter and the recycled aggregate content. These parameters were chosen because of their strong influence over the local bond behaviour. The influence of these parameters was accounted for by way of coefficients, either newly created or previously existing and calibrated.

Experimental results and data treatment

Before the calibration process, each author's experimental bond stress-slip results were collected with the data regarding the bond-related parameters. Table 1 contains the relevant information regarding the characteristics of each experimental test series performed.

Regarding Louro (2014), the specimens are identified by their reinforcement batch (i.e. A, B, AT or BT), followed by the type of concrete used and lastly, the diameter of the main bar. C1 and C2 refer to the target strength classes C30/37 and C50/60, respectively. It should also be noted that the specimens which involved cyclic loading or where yielding of the reinforcement occurred were excluded from the data considered in the present work.

Freitas's (2016) experimental campaign specimens are identified by the type of concrete (i.e. C250, LBC125 or LBC75), followed by the type of steel and the bar's diameter. In this case, the identifiers *A* and *i* correspond to steel and stainless steel, respectively. Finally, Pereira's (2019) experimental campaign is divided into LBC and LCRAC concrete specimens. LBC series includes a numeric identifier ranging from 0,82 to 0,86, which is related to their packing density and a second identifier concerning the optimisation packing curves used (i.e. Alfred or Faury). In contrast, LCRAC series are identified regarding the total percentage of RA content.

The concrete compressive strength data from Louro (2014) and Freitas (2016) was converted from $f_{cm,cube}$ to f_{cm} using equation (1), following the same criteria applied by Pereira (2019).

$$f_{cm} = 0.82 * f_{cm,cube} \quad (1)$$

Each author's local bond stress values were normalised according to the same criteria, considering the non-linear influence of the concrete compressive strength over bond behaviour, as is shown in expression (2). This step was essential since the authors used different criteria for calculating τ_d; Freitas (2016) used the recommendations from Annex D of EN 10080 (2005), which indicate $f_{cm,28}/f_{cm,j}$, whereas Louro (2014) and Pereira (2019) followed the recommendations of *fib* Model Code 2010, which indicates $\sqrt{f_{cm,28}/f_{cm,j}}$. Afterwards, the mean values of the bond stress-slip curve were calculated for each series, which would serve as the target for the calibration process to be developed. τ_b is the experimentally measured bond stress prior to normalisation.

$$\tau_d = \tau_b \cdot \sqrt{\frac{f_{cm,28}}{f_{cm,j}}} \quad (2)$$

Table 1 – Characteristics of the POT specimens of each testing series.

	Test Series	Nº SPEC	d (mm)	$f_{cm,28}$ (MPa)	σ	f_R	c (mm)	a (mm)	$RA_{<c}$	$RA_{\geq c}$
Louro (2014)	A_C1_16	3	16	38.25	0.796	0.081	9.97	1.29	0.00	0.00
	B_C1_16	3			0.834	0.099	9.87	1.58		
	AT_C1_16	3			0.796	0.080	9.95	1.28		
	BT_C1_16	3			0.834	0.098	9.87	1.59		
	A_C2_16	3		57.80	0.780	0.081	9.97	1.29		
	AT_C2_16	3				0.080	9.95	1.28		
	A_C1_25	6	25	38.25	0.796	0.096	14.35	2.22		
	B_C1_25	6				0.101	14.47	2.41		
	AT_C1_25	3			0.834	0.097	14.37	2.27		
	BT_C1_25	3				0.101	14.45	2.41		
	A_C2_25	3		57.80	0.780	0.096	14.35	2.22		
	B_C2_25	6				0.097	14.47	2.41		
Freitas (2016)	C250_A12	5	12	32.64	0.810	0.082	7.80	1.07	0.00	0.00
	C250_i12	4				0.058	6.67	0.67		
	LBC125_A12	5		27.12	0.860	0.082	7.80	1.07		
	LBC125_i12	5				0.058	6.67	0.67		
	LBC75_A12	5		17.77		0.082	7.80	1.07		
	LBC75_i12	5				0.058	6.67	0.67		
	C250_A16	5	16	32.64	0.810	0.066	10.80	1.18		
	C250_i16	5					10.18	1.06		
	LBC125_A16	5		27.12	0.860		10.80	1.18		
	LBC125_i16	5					10.18	1.06		
	LBC75_A16	5		17.77			10.80	1.18		
	LBC75_i16	5					10.18	1.06		
Pereira (2019)	LBC_0,86_Alfred	4	12	29.70	0.860	0.073	7.7	0.95	0.00	0.00
	LBC_0,84_Alfred	5		20.20	0.840					
	LBC_0,82_Alfred	5		14.70	0.820					
	LBC_0,86_Faury	5		26.90	0.860					
	LCRAC_30	5		24.50	0.840					0.30
	LCRAC_55	5		19.30					0.10	0.45
	LCRAC_80	5		15.50					0.34	0.46

Bond stress slip models

Currently, *fib* Model Code 2010 establishes a local bond stress-slip relationship for monotonic loading of ribbed bars in the elastic range of steel ($\varepsilon_s < \varepsilon_{s,y}$), and accounts for diferent types of failure, as established in Figure 1.

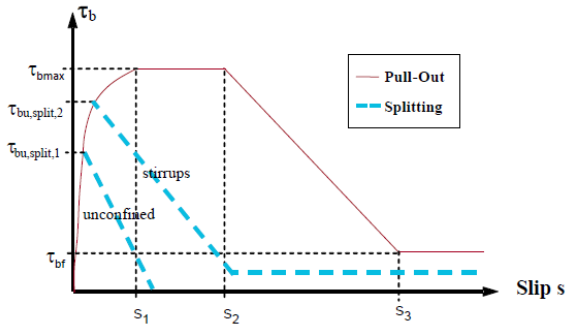

Figure 1 – Bond stress-slip relationship for monotonic loading, adapted from fib Model Code 2010.

The *fib* Model Code 2010 model performs the calculation of the bond stress values τ_b according to the diferent stages of the bond stress-slip curve, as shown by the expressions (3), (4), (5) and (6).

$$\tau_b = \tau_{bmax} \cdot \left(\frac{s}{s_1}\right)^{\alpha}, \quad for\ 0 \leq s \leq s_1; \tag{3}$$

$$\tau_b = \tau_{bmax}, \quad for\ s_1 \leq s \leq s_2; \tag{4}$$

$$\tau_b = \tau_{bmax} - (\tau_{bmax} - \tau_{bf}) \cdot \frac{s - s_2}{s_3 - s_2}, \quad for\ s_2 \leq s \leq s_3; \tag{5}$$

$$\tau_b = \tau_{bf}, \quad for\ s_3 < s; \tag{6}$$

Where, τ_{bmax} is the bond strength for the pull-out failure, $\tau_{bu,split,1}$ and $\tau_{bu,split,2}$ are the bond strength for the splitting failures, τ_{bf} is the reference residual bond stress due to bond friction, s_1, s_2 and s_3 are the slip for the beginning and end of the bond strength plateau and the beginning of the residual bond stress, respectively, f_{cm} is the mean concrete compressive strength, c is the clear distance between ribs, α is the coefficient that characterizes the $\tau_b - s$ relationship of the ascending branch.

Based on the conditions defined by *fib* Model Code 2010 for bond behaviour of bars with a pull-out failure and good bond conditions (Table 2), several authors have proposed new models that incorporate coefficients that account for the influence of several parameters well-known in the literature to influence the bond behaviour. Such are the cases of Louro (2014), Freitas (2016) and Pereira (2019). The bond-related parameters considered were the bond index, the packing density and the RA content of size inferior to the rib spacing. These parameters are important for the bond performance of bars embedded in OC/LBC/LCRAC. Table 3 displays the bond models from the various authors.

Table 2 – Parameters of the bond stress-slip model for ribbed bars presented in fib Model Code 2010.

	Pull-out failure + Good bond conditions
τ_{bmax}	$2.5 \cdot \sqrt{f_{cm}}$
s_1	$1.0\ mm$
s_2	$2.0\ mm$
s_3	c
α	0.4
τ_{bf}	$0.4 \cdot \tau_{máx}$

Table 3 – Bond models proposed by Louro (2014), Freitas (2016) and Pereira (2019) for the case of pull-out failure and good bond conditions.

	Louro (2014)	*Freitas (2016)*	*Pereira (2019)*
τ_{bmax}	$\beta \cdot \sqrt{f_{cm,cube}}$	$2.5 \cdot \sqrt{f_{cm,cube}} \cdot\ k_{f_R} + k_\sigma$	$2.5 \cdot \sqrt{f_{cm}} \cdot\ \eta_{f_R} \cdot\ \eta_\sigma \cdot\ \eta_{RA_{<c}}$
$\beta \mid k_{f_R} \mid \eta_{f_R}$	$\begin{cases} 2.65, & if\ f_R > 1.6 \cdot f_{R,min} \\ 2.35, & if\ f_R \leq 1.6 \cdot f_{R,min} \end{cases}$	$\frac{f_R}{0.056}$	$4.757 \cdot f_R + 0.8785$
$- \mid k_\sigma \mid \eta_\sigma$	-	$100 \cdot (\sigma - 0.81)$	$7.927 \cdot \sigma - 5.408$
$- \mid - \mid \eta_{RA_{<c}}$	-	-	$1 - 0.972 \cdot RA_{<c}$
s_1	$\begin{cases} 0.5, & if\ f_R > 1.6 \cdot f_{R,min} \\ 1.0, & if\ f_R \leq 1.6 \cdot f_{R,min} \end{cases}$	1.0	$1.0 - 5 \cdot (\sigma - 0.82), \quad for\ \sigma \geq 0.82$
s_2	$\begin{cases} 1.5, & if\ f_R > 1.6 \cdot f_{R,min} \\ 2.0, & if\ f_R \leq 1.6 \cdot f_{R,min} \end{cases}$	2.0	$2.0 - 5 \cdot (\sigma - 0.82), \quad for\ \sigma \geq 0.82$
s_3	c	c	c
α	0.4	0.4	$0.4 - 4 \cdot (\sigma - 0.82), \quad if\ \sigma \geq 0.82$
τ_{bf}	$0.4 \cdot \tau_{bmax}$	$0.4 \cdot \tau_{bmax}$	$0.3 \cdot \tau_{bmax}, \quad for\ LBC/LCRAC$ $0.4 \cdot \tau_{bmax}, \quad for\ OC$

Calibration Methodology

The calibration of the bond strength parameter was performed through an iterative method which consisted of the following steps:

1. First, the *fib* Model Code 2010 expression for bond strength was multiplied by a set of coefficients φ_j [expression (7)]. Each coefficient had a physical significance and related to the influence of a certain bond-related parameter.

$$\tau_{bmax} = 2.5 \cdot \sqrt{f_{cm}} \cdot\ \prod_{j=1}^{n} \varphi_j \qquad (7)$$

2. The initial expression for each φ_j coefficient was either obtained from previous bond models or created through analysis of the experimental data. The goal of the iterative method was to refine the initial expressions of the φ_j coefficients by weighing their isolated influence over the data relative to the mean bond strength of each pull-out test series. For example, at the first iteration step, the preponderance of the coefficient φ_1 is weighed through the calculation performed in the expression (8).

$$\tau_{dmax} = 2.5 \cdot \sqrt{f_{cm}} \cdot\ \prod_{j=1}^{n} \varphi_j\ <=> \quad \varphi_1 = \tau_{dmax} / 2.5 \cdot \sqrt{f_{cm}}\ \cdot\ \prod_{j=2}^{n} \varphi_j \qquad (8)$$

3. The data regarding the preponderance of the weighed coefficient is gathered, and a graphic containing a regression line of the results is plotted. If the plotted regression line proves to better adapt to the isolated influence of the coefficient than the first (or previous) equation of the coefficient, the equation is 'stored' as the new expression for the coefficient, thus ending the present iteration step.

4. In each following iteration step, the same process is performed for the subsequent coefficient, using an equal process, although considering the replacement equation(s) stored for the previous iterated coefficient(s).
5. Once all coefficients have been iterated once, the process restarts until otherwise a pre-established convergence criterion is met.

At each iteration of a given coefficient φ_j the goodness-of-fit measure value R^2 regarding the plotted regression line tends to converge. Once the differences between R^2 values from the previous and the subsequent iteration of all coefficients were equal to or lower than 0.001, then the calibration was deemed complete, as no significant improvement was expected to be obtained.

The remaining parameters of the bond stress-slip model, s_1 , s_2 and τ_{bf}, were calibrated through direct relationships with the parameters that showed to be the most influential.

Calibration results

The outcome of the calibration of the new local bond stress-slip model for steel reinforcement embedded in OC, LBC or LCRAC under good bond conditions for pull-out failure is presented in

Table 4. Note that τ_{bmax} is the bond strength, φ is the coefficient for the influence of the identified bond-related parameter, s_1 and s_2 are the limit slip values of the bond strength plateau, s_3 is the slip value for the beginning of the bond's residual capacity, α is the coefficient that characterizes the $\tau_b - s$ relationship of the ascending branch and τ_{bf} is the residual bond stress due to bond friction.

Table 4 – Proposed local bond stress–slip model.

τ_{bmax} [MPa]	$2.5 \cdot \sqrt{f_{cm}} \cdot \varphi_{f_R} \cdot \varphi_\sigma \cdot \varphi_d \cdot \varphi_{RA_{\geq c}} \cdot \varphi_{RA_{<c}}$
φ_{f_R}	$4.757 \cdot f_R + 0.8785$
φ_σ	$117.17 \cdot \sigma^2 - 188.24 \cdot \sigma + 76.397$
φ_d	$-0.0292 \cdot d + 1.4634$
$\varphi_{RA_{\geq c}}$	$-2.2446 \cdot RA_{\geq c}^2 + 1.4731 \cdot RA_{\geq c} + 0.9579$
$\varphi_{RA_{<c}}$	$4.038 \cdot RA_{<c}^2 - 2.4333 \cdot RA_{<c} + 1.2152$
s_1 [mm]	$0.05 \cdot d + 0.15$
s_2 [mm]	$0.05 \cdot d + 1.15$
s_3 [mm]	c
α	0.4
τ_{bf} [MPa]	$0.5164 \cdot \tau_{bmax} - 1.017, \quad for\ OC$
	$0.3826 \cdot \tau_{bmax} - 0.9094, \quad for\ LBC/LCRAC$

FINITE ELEMENT MODELLING OF THE BOND BEHAVIOUR

The finite element models were built using the software ATENA developed by *Červenka Consulting s.r.o.*. This choice of software was based on its ability to model the bond behaviour by assigning reinforcement elements with a bond function through a so-called *reinforcing bar with bond* system.

Concrete elements were modelled using the material CC*3DNonLinCementitious2.* This material model is based on fracture mechanics, plasticity and damage and combines constitutive laws for tensile and compressive behaviour. The reinforcing bars were modelled using the material *CCReinforcement,* which considers the steel behaviour according to a bilinear stress-strain law with hardening. The bond behaviour was modelled with the material *CCReinforcementBondModel*, which requires the definition of a bond stress-slip function

The loading and support conditions are applied through the loading history, which defines all actions that occur during the processing phase of the numerical analysis and consists of several analysis steps, each one combining a set of load cases (i.e. the support conditions plus prescribed deformation/applied forces). Furthermore, the ATENA software defines the total actions by the integral in time of the force increments by applying a solution method such as the Newton-Raphson method, which was employed in all analyses.

Description of the finite element models

The pull-out model was created to replicate the test specimens of the experimental campaigns of Louro (2014), Freitas (2016) and Pereira (2019). The initial intent of this model was to perform the numerical calibration of a new bond stress-slip law concerning the local bond behaviour of various concrete types. However, the realisation that the modelling approach chosen was not suited to this purpose led to a change in the objectives. Hence, the pull-out model showed that it is possible to successfully model local bond behaviour and compare the experimental results from the various campaigns with the theoretical bond models incorporated into the numerical modelling.

In addition, the approach utilised to model the local bond behaviour of the pull-out model was then employed in the modelling of two beam models with different reinforcement configurations. By modelling these structures, utilizing the theoretical bond models for local bond behaviour, it was possible to study the bond behaviour of reinforcing bars with long embedded lengths and the bond failure occurring around the anchorage/lap-splice zones of the reinforcement.

Pull-out model

Four reference models were designed with geometrical properties similar to those of the test specimens. Furthermore, these models were divided into four groups to account for the slight differences between the specimens produced by each author: the Standard pull-out model (with diameters of 12 and 16 mm) and the Modified pull-out model (with diameters of 16 and 25

mm). Each reference model mainly differs in dimensions and represents all the test series performed with similar geometry. The material properties of each reference model were subsequently changed to replicate the characteristics of a given test series and consequently conduct the intended non-linear structural analysis.

The model's geometric definition was performed in the *ATENA 3D* user interface and started with creating ME for the concrete parts of the pull-out test and 1D discrete truss elements to represent the reinforcing bars. Additionally, to model the reinforcement as embedded or disconnected to the surrounding concrete, separate concrete elements were created: two for the Standard and three for the Modified models; The same was applied to the reinforcement elements, which were created with various segments to account for the different bond interfaces. Lastly, an auxiliary cube was created and connected to the main reinforcement element enabling the prescribed displacement to be applied to the pull-out model. Figure 2 presents a view of both the Standard and the Modified models during the pre-processing stage.

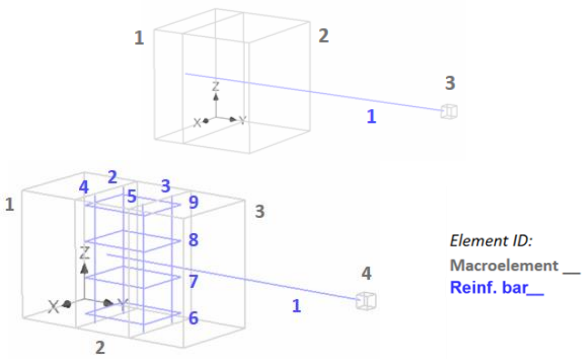

Figure 2 – 3D view of the Standard (top) and Modified (bottom) models.

Regarding the auxiliary element used for loading the model, the material *CC3DElastIsotropic* was chosen to replicate a linear elastic isotropic behaviour.

The definition of the bond material was always defined by the user considering the bond models previously mentioned in this work and the new calibrated model. Lastly, in the case of the transverse reinforcing bars, no bond material was assigned to them (i.e. perfect connection set by default was considered), given that it would not be relevant to the analysis.

The loading history of the pull-out model consists of two load cases: a prescribed displacement and the support conditions. Loading of the model was performed through a prescribed displacement of 0.20 mm along the axial direction of the main reinforcement, prescribed to the surface of the auxiliary element. Thus, the analysis was set to run for 100 steps using the Newton-Raphson method with a limit of 40 iterations per step to reach a final displacement of 20 mm. Also, the support conditions consisted of restraining the translations, in all directions, of the concrete element's surface closest to the loaded end of the reinforcement. Additionally, translations in the X and Z directions were restrained in the loaded surface of the auxiliary element to avoid any lateral movements when under load.

The mesh generated for the reference models consisted of different finite element types: the concrete regions were meshed using linear hexahedral elements, whereas the auxiliary cube was roughly meshed using linear tetrahedral elements.

Beam models

The beam models were conceived as simply supported beams of small cross-section and distinct reinforcement layouts: the first with straight anchored bars [Straight Anchorage Beam (SAB) model] and the second with lap-spliced bars [Lap-Splice Beam (LSB) model]. The goal of these beams was to evaluate the development length that their reinforcement would require to resist a bending action whilst also varying the bond function assigned to the reinforcement. Thus, these beam models were the basis of a parametric study investigating the influence of the local bond behaviour on the reinforcement development length on beams with low binder concrete and low cement recycled aggregate concrete.

The geometric definition of both beam models was performed in the *GiD* user interface and can be summarised by the creation of the concrete body followed by the rectangular support/loading plates and, finally, the truss elements for the reinforcing bars. Figure 3 and Figure 4 provide a graphical description of the geometry of the SAB and LSB models, respectively.

The parameters used for the concrete material of both the SAB and LSB models were those catalogued in Eurocode 2 for a C25/30 concrete with mean values, and the reinforcement elements were assigned a steel material with the mean values of a B500C class steel. The support/loading plates were assigned the same material used in the auxiliary element of the pull-out models. The bond model assigned to the reinforcing bars was defined by the user as intended. The slip was restrained where the bars are contacting the beam's lateral surfaces to simulate the restrained slip of a hooked anchorage.

The loading history of the SAB model consists of a single point load applied at the centre point of the top plate and two simple supports applied along a centre line parallel to the X-axis on the bottom plates. The analysis was performed using the Newton-Raphson method and was set to run for 100 steps, with a limit of 40 iterations per step, until the loading value reached 80 kN.

The loading history of the LSB model consists of two point loads applied at the centre points of the top plates and two simple supports applied along a centre line parallel to the X-axis on the bottom plates. Once again, the analysis was performed using the Newton-Raphson method, and for this model, it was set to run for 100 steps, with a limit of 40 iterations per step, until the loading value at each plate reached 40 kN. The mesh of both beam models was generated with linear

hexahedral elements in the concrete region and tetrahedral elements divided loading/support plates.

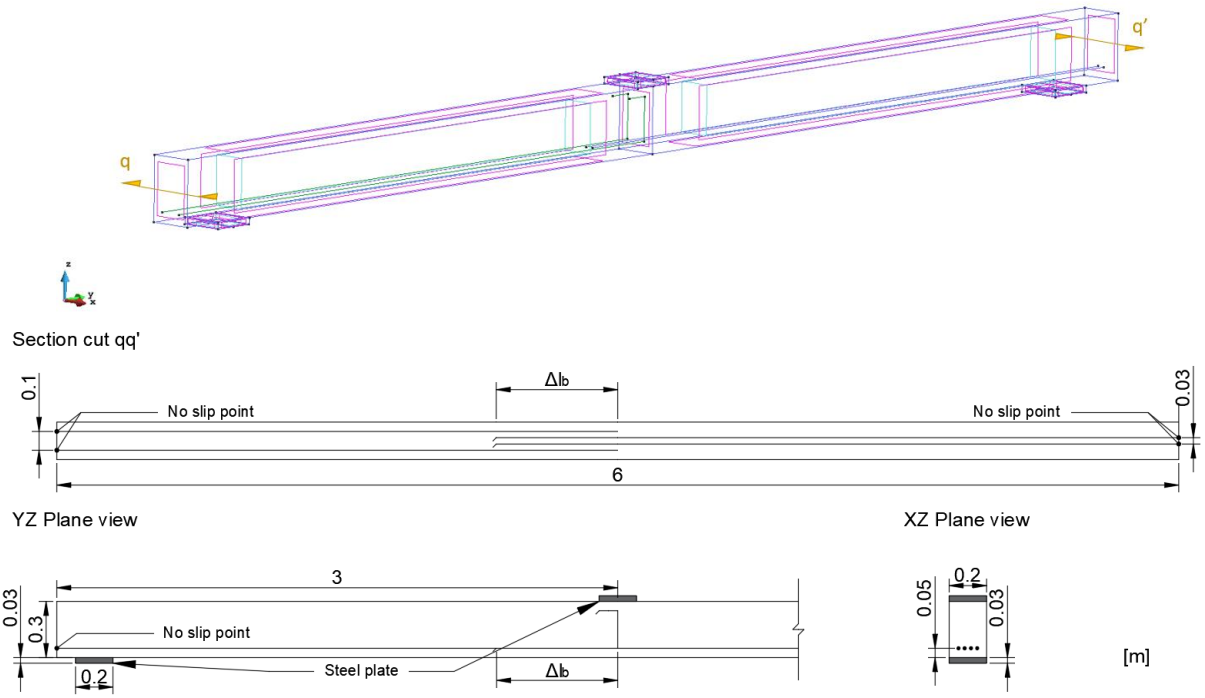

Figure 3 – Geometry of the straight anchorage beam model (SAB model).

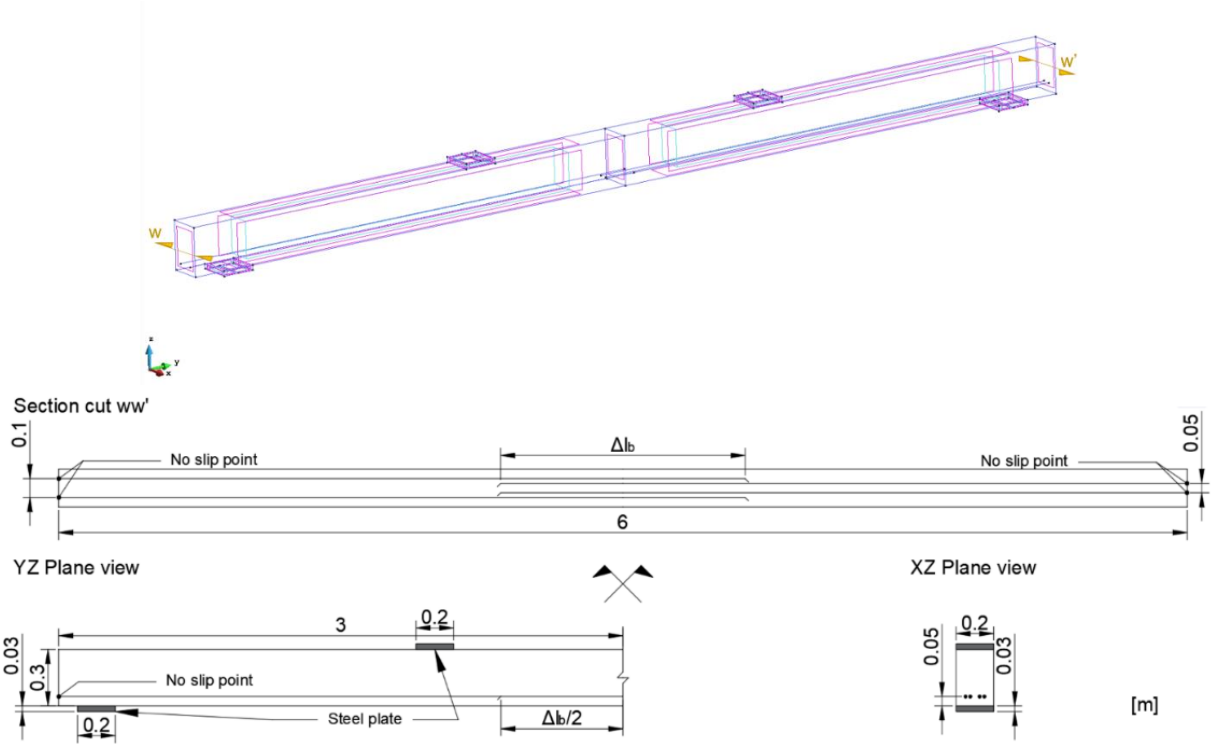

Figure 4 – Geometry of the lap-splice beam model (LSB model).

DISCUSSION OF THE NUMERICAL ANALYSIS RESULTS

Pull-out model

The four reference models were subjected to a validation process to ensure that the obtained results were in accordance with what was expected from this type of experiment. The models were tested during the validation process using a C30/37 concrete material, a B500C steel material and considering the *fib* Model Code 2010 bond model.

Overall, the models successfully captured the bond behaviour of a short length embedded bar. Results showed that the bond stress starts to increase at the beginning of the embedded length, quickly reaching a

mean bond stress value that remains the same throughout the remaining bonded length.

Comparison between experimental and numerical results

The deviation to accuracy error regarding the prediction of bond strength with the new calibrated model was calculated for each test series and compared to the calculations performed for the existing models. From a statistical point of view, this comparison showed that the calibration process brought substantial improvements to the prediction of bond strength of OC/LBC/LCRAC. Results are presented in Table 5 where Δ_{max} indicates the maximum positive error among all series, Δ_{min} the maximum negative error, $\Delta_{max} + |\Delta_{min}|$ indicates the range between the maximum positive and negative error, Δ_{mean} is the mean error and Δ_{med} the median error.

Table 5 – Accuracy to deviation error data relative to the bond strength parameter.

	fib Model Code 2010	*Louro (2014)*	*Freitas (2016)*	*Pereira (2019)*	*New Model*
Δ_{max}	104.32%	96.83%	12.22%	30.98%	24.99%
Δ_{min}	-8.04%	-21.44%	-56.00%	-42.15%	-22.51%
$\Delta_{max} + \lvert\Delta_{min}\rvert$	112.36%	118.27%	68.22%	73.13%	47.50%
Δ_{mean}	39.30%	31.48%	-17.20%	-1.48%	0.00%
Δ_{med}	33.30%	28.41%	-10.62%	0.38%	-0.01%

Beam models

The numerical beam models were created to extrapolate the successful modelling of the local bond behaviour into a scenario of a conceptual structural member, where the embedded length of the reinforcement is no longer short. The second intention behind the creation of the beam models was to study the influence that different local bond strength levels have on the anchorage/lap-splice length of the reinforcement. This exercise is of special relevance since it could provide information regarding the use of different concrete types as well as of bars with different characteristics and their impact on the structural behaviour, where development lengths are concerned.

Consequently, the analysis was performed using either the fib Model Code 2010 bond model or the calibrated model proposal to simulate the bond behaviour. Additionally, the analysis was based on a set of reference values for the studied bond-related parameters, which would then be varied in order to study their influence on the development length of the bars. The reference set of parameters was intended to match the characteristics of an LBC with medium compressive strength. Additionally, the reinforcing bars used always maintain a diameter of 16 mm, which is the middle ground from the experimental range of diameters that comprised the data set used to calibrate the proposed bond model. From this reference set of parameters, variations were then introduced to take into account the maximum values of the studied range of each bond-related parameter to provide some sense of how influential these can be to the variation in the development length of the reinforcement. In total, six different bond strength levels were analysed, which are identified in Table 6.

.

Table 6 – Variations of the bond model used in the SAB and LSB models.

Bond model	*Parameters*	f_{cm} *(MPa)*	f_R	σ	*d (mm)*	$RA_{<c}$	$RA_{\geq c}$	τ_{bmax} *(MPa)*
fib MC2010	Reference	33	0.058	0.82	16	0.00	0.00	14.36
New model	Reference		0.058	0.82		0.00	0.00	**15.87**
	Variation 1		0.058	0.82		**0.34**	0.00	11.16
	Variation 2		**0.101**	0.82		0.00	0.00	18.68
	Variation 3		0.058	0.82		0.00	**0.46**	19.22
	Variation 4		0.058	**0.86**		0.00	0.00	22.48

For each variation introduced in the bond function assigned to the bars of the beam model, an iterative exercise was performed to assess the development length necessary for the beam to avoid failure due to insufficient bond resistance. Thus, this exercise consisted in running several analyses for each set of parameters, where the length of the bars would vary 5 mm at a time. During the analysis, the axial stress in the bars was monitored, as well as the bond stress-slip response at the end of the reinforcement. The anchorage length for a given bond level would then be assessed by registering at which bar length the yielding of the steel would occur previously to the maximum bond stress at the end of the bars being reached. The results of this process were documented and will be discussed in the following sections.

Simple Anchorage beam model

The consequential results of this process are presented in Table 7, and Figure 5 illustrates the evolution of the necessary anchorage length according to the bond strength level employed.

Table 7 – SAB model: anchorage length results according to the bond strength level.

Bond model	*Parameters*	⇔	τ_{bmax} *(MPa)*	$\Delta\ \tau_{bmax}$ *(%)*	*Anchorage length (mm)*	$\Delta\ l_b$ *(%)*
fib MC2010	Reference	-	14.36	0%	225	0%
New model	Reference	-	15.87	11%	200	-11%
	Variation 1	$RA_{<c}=0 \rightarrow 0.34$	11.16	-22%	280	24%
	Variation 2	$f_R=0.580 \rightarrow 0.101$	18.68	30%	150	-33%
	Variation 3	$RA_{\geq c}=0 \rightarrow 0.46$	19.22	34%	150	-33%
	Variation 4	$\sigma=0.82 \rightarrow 0.86$	22.48	57%	145	-36%

** Δ refers to variation relative to the fib Model Code 2010 bond model's results*

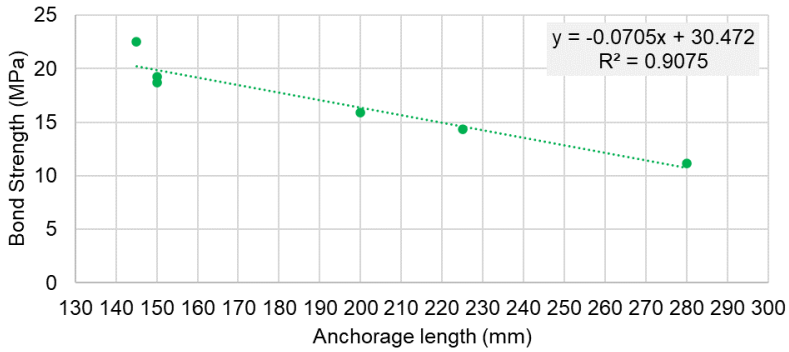

Figure 5 – SAB model: bond strength versus anchorage length.

Concerning the reference set of parameters, a first observation can be made that the use of the new bond model requires less steel than the one from fib Model Code 2010. The difference in anchorage length between the two models was 25 mm, accounting for an 11% variation in anchorage length, coincidentally the same as the variation in bond strength between the models. Comparison between these cases is useful since it provides an example of the differences in material usage obtained from using a rather conservative bond model or a more precise model; however, the number of results obtained is very limited, and so any conclusion that is reached should consider this factor (i.e. a much larger number of data would be necessary to affirm with certainty how much is the impact of using different bond models). Secondly, observing parameter variation 1, which concerns the use of 34% of $RA_{<c}$, it is very clear that the loss in bond strength is very negative to the anchorage requirements: a difference of 80 mm and the anchorage length varying once again linearly with the bond stress. Thirdly, it was interesting to observe that parameter variation 3 (regarding 46% of $RA_{\geq c}$) seems to be as much beneficial as the use of ribbed bars with a high bond index (parameter variation 2); this is, both registered the same anchorage length given their similar bond strength levels. However, as mentioned previously, results regarding the prediction of bond strength in LCRAC should be taken with some caution.

The best results were present when using an LBC with a high packing density (parameter variation 4), which provided the shortest anchorage length. Nonetheless, it should be noted that contrary to the registered tendency of previous parameter variations, where the reduction in anchorage length seems to vary linearly with the bond strength, the present case presented only a 36% reduction in bar length when bond strength increased 57% (comparatively to the fib Model Code 2010 bond model).

Lap-splice beam model

The consequential results of the lap-splice length evaluation process are presented in Table 8, and Figure 6 depicts the evolution of the lap-splice length according to the bond strength level.

Table 8 – LSB model: lap-splice length results according to the bond strength level.

Bond model	*Parameters*	⇔	τ_{bmax} *(MPa)*	$\Delta\ \tau_{bmax}$ *(%)*	*Lap-splice length (mm)*	$\Delta\ l_b$ *(%)*
fib MC2010	Reference	-	14.36	0%	250.0	0%
New model	Reference	-	15.87	11%	230.0	-8%
	Variation 1	$RA_{<c}=0 \rightarrow 0.34$	11.16	-22%	270.0	8%
	Variation 2	$f_R=0.580 \rightarrow 0.101$	18.68	30%	220.0	-12%
	Variation 3	$RA_{\geq c}=0 \rightarrow 0.46$	19.22	34%	220.0	-12%
	Variation 4	$\sigma=0.82 \rightarrow 0.86$	22.48	57%	180.0	-28%

** Δ refers to variation relative to the fib Model Code 2010 bond model's results*

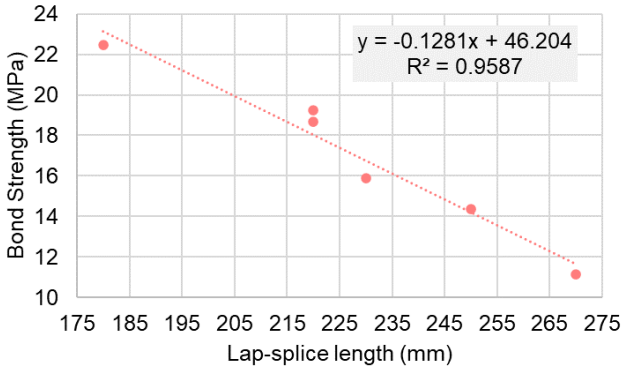

Figure 6 – LSB model: bond strength vs lap-splice length.

As was observed for the anchorage length in the SAB model, the lap-splice length seems to vary linearly with the bond strength level of the reinforcement. The linear regression line for these results has a higher goodness-of-fit value than the previous ones (R^2=0.9587 versus 0.9075), which is undoubtedly due to the parameter variation 4 not disrupting the tendency established by the previous variation, as was the case in the SAB model. However, this relationship shows some differences from the one observed previously, with variation in bond strength leading to smaller changes in bar length. This fact is quite noticeable in the parameter variations 2 and 3, where a difference of around 30% in bond strength (comparatively to the fib Model Code 2010 bond model) equated to less than half of that value in the lap-splice length variation.

CONCLUSIONS

The main outcome of the present dissertation was the calibrated bond model for OC/LBC/LCRAC. This new bond model focused on including the influence of a broad range of bond-related parameters, already established in the literature as capable of affecting the bond performance but not yet properly quantified in conjunction with other bond parameters. The new model and its created coefficients are presented in Table 2.

The comparison between the numerical and experimental results enabled the evaluation of the various bond models. Overall, the calibrated bond model was able to provide more accurate results than the pre-existing models, with its mean deviation to accuracy error being 0% compared to 39.20, 31.48, -17.20 and -1.48% for the models of fib Model Code 2010, Louro (2014), Freitas (2016) and Pereira (2019), respectively. Although the mean error of the calibrated model is very similar to that of the model from Pereira (2019), the new model was able to reduce the difference between the maximum positive and negative error (47.50% compared to 73.13%) and also provides more accurate results, despite all the mentioned shortcomings and the occasional non-conservative prediction.

Nonetheless, the successful modelling of the POT enabled then the modelling of the local bond behaviour to be extrapolated to two different beam models. These beam models permitted the evaluation of anchorage and lap-splice lengths by using the local bond stress-slip model to prescribe the bond behaviour to the reinforcement. Furthermore, the results from the beam models showed that by considering the different bond resistance capacity that comes with the use of different concrete types and reinforcing bars, the length of reinforcement needed in the anchorage/lap-splice zones is affected. Both models exhibited a positive linear relationship between the bond strength variation and the anchorage/lap-splice length variation. Thus, the use of properly conceived ecological concrete mixtures such as LBC and LCRAC are shown in this exercise to have an ability to improve the sustainability of the construction industry but also to improve the structural performance where bond performance is concerned. However, it should be safeguarded that the restricted number of obtained results lend to this exercise a mere exploratory nature, and a bigger data pool would be required for the drawn conclusions to be more certain and trustworthy.

REFERENCES

European Aggregates Association (2022). *31st of May 2022*, https://uepg.eu/pages/facts

European Committee for Standardization (2005). 'Steel for the reinforcement of concrete - Weldable reinforcing steel - General' (EN 10080:2005).

Federation internationale du beton. (2010). *fib Model Code for Concrete Structures 2010*. Ernst & Sohn.

Flower, D. J. M., and Sanjayan, J. G. (2007). 'Green house gas emissions due to concrete manufacture'. *The International Journal of Life Cycle Assessment*, 12(5), 282–288.

Freitas, E. R. (2016). 'Bond between stainless steel bars and low binder concrete' (in Portuguese), *Master's Thesis, Instituto Superior Técnico, Lisbon*.

Kosmatka, S. H., Kerkhoff, B., and Panarese, W. C. (1996). *Design and Control of Concrete Mixtures, EB001*. *Design and Control of Concrete Mixtures*.

Lehne, J., and Preston, F. (2018). 'Chatham House Report - Making Concrete Change Innovation in Low-carbon Cement and Concrete'

Louro, A. S. (2014). 'Characterization of bond of ribbed bars subjected to repeated and alternating actions' (in Portuguese), *PhD Thesis, Universidade Nova de Lisboa, Lisbon*.

Pereira, T. (2019). 'Bond between steel bars and low binder concrete with the incorporation of recycled aggregates' (in Portuguese), *Master's Thesis, Instituto Superior Técnico, Lisbon*.